Journal of Mathematical Modeling
Vol. 13, No. 4, 2025, pp. 886-899. Research Article

JMM

Numerical solution of obstacle problem by using the mesh-free radial point interpolation method

Ahmed Awad Nasser[†], Masoud Allame[†*], Habeeb Abed Kadhim Aal-Rkhais[‡], Majid Tavassoli-Kajani[†]

[†] *Department of Mathematics, Isfahan (Khorasgan) branch, Islamic Azad University, Isfahan, Iran*
[‡] *Department of Mathematics, College of Computer and Mathematics, University of Thi-Qar, Iraq*
Email(s): hmeadaoad8657@gmail.com, allame@khuisf.ac.ir, habeebk@utq.edu.iq, mtavassoli@khuisf.ac.ir

Abstract. The obstacle problem is a well-known type of elliptic variational inequality that originally arose from contact issues in solid mechanics. The solutions to the obstacle problem often have irregularities along a free boundary, which can be effective in designing an appropriate numerical method for these problems. In this paper, we present a mesh-free method based on the radial point interpolation method for numerically solving an obstacle problem. In the proposed method, the radial point interpolating shape functions are utilized in the global weak form of the obstacle problem, based on the element-free Galerkin method. This approach is combined with an active set strategy to address the obstacle problem. One of the key benefits of the proposed method is its independence from any mesh of the computing domain, along with its straightforward implementation and high numerical stability. To ensure the efficiency of the presented method, we have investigated the convergence of the proposed method. The obtained numerical results confirm the theoretical achievements and demonstrate the method's effectiveness and accuracy.

Keywords: Obstacle problem, variational inequality, radial points interpolation method, meshfree method.
AMS Subject Classification 2010: 65N99, 35J86.

1 Introduction

In mathematical view, the obstacle problem can be formulated as an *elliptic variational inequality*. A variational inequality is an inequality involving a functional that must hold for all values within a convex subset of a space [23]. For the mathematical modeling of the obstacle, consider the area $D \subset \mathbb{R}^n, n = 1,2$ and its boundary ∂D, where the elastic membrane is located on D. The membrane position is denoted

*Corresponding author
Received: 7 March 2025 / Revised: 2 May 2025 / Accepted: 3 June 2025
DOI: 10.22124/jmm.2025.29905.2671

© 2025 University of Guilan

by y and the force applied to it is denoted by $g \in C(D)$. Also, the surface of the obstacle situated on D is denoted by $z \in C(D)$. Then by definition of the range of admissible changes for the desired elastic membrane as

$$\mathscr{O} := \left\{ h \in H^1(D) \mid \; h \le z \text{ a.e. in } D \;\&\; h\,|_{\partial D} = y_b \right\}, \tag{1}$$

the model of the obstacle problem will lead to the finding $y \in \mathscr{O}$ such that [13]:

$$(\nabla y, \nabla (y-u)) \le (g, y-u) \quad \forall u \in \mathscr{O}. \tag{2}$$

Here, the notation $H^1(D)$ is used to refer the Sobolov function space of order 1 from $L^2(D)$ and its inner product denoted by $(\cdot,\cdot)$. The problem (1)-(2) is an elliptic variational inequality, since the functional inequality (2) must hold for all values of $u \in \mathscr{O}$. This problem is recognized as a *free boundary problem* in science [5].

Due to the existing a priori unknown free boundary between contact and non-contact sets, special methods are required to solve this problem numerically. Semi-smooth Newton algorithm [7,24], interior point strategy [29] or active set algorithm [12] are some of the famous method to tackle the obstacle problem. These algorithm combined with some traditional numerical method for discretization issue. Several numerical methods have been used for this purpose so far. Finite difference (FD) methods [19] and finite element methods (FEM) [2,3] are most popular numerical methods which are used for solving obstacle problem. Moreover, more accurate numerical methods, such as wavelets methods [14] and pseudo spectral method [15] have also been utilized for this purpose. Additionally, in [16,30] the discrete Galerkin method (DGM) has been employed to tackle this issue.

Due to the simplicity and flexibility in the implementation, compatibility with non-rectangular domains, research on solving problems with mesh-free methods has been increasing [1,27]. Among this family of methods, the following examples can be mentioned that have been used to solve the obstacle problem: the meshless local Petrov-Galerkin method in [26], the generalized finite differences in [4] and the element-free Galerkin method in [18]. Some of these methods are based on obtaining the weak form of the problem. Where the numerical integration can ultimately be used to derive a linear system, and solving this system will yield an approximation of the solution to the problem [9].

In this paper, we seek to design a mesh-free method based on the global weak form. The element-free Galerkin method (EFGM) is one of the most important methods in this family of methods. In EFGM, the moving least squares (MLS) shape functions are employed as the test and trial functions in Galerkin schema [6]. The main disadvantage of these basic functions is the lack of the delta Kronecker property. For this reason, the essential boundary conditions cannot be implemented directly in this method. Therefore, designing a method in the form of a global weak form with bases having the Kronecker delta property became the subject of further research. To overcome this weakness, the use of the radial point interpolation method (RPIM) shape functions instead of MLS shape function is recommended [20,21].

In this work, we will present a meshless method based on the use of the RPIM to solve the obstacle problem. Also, a combination of this meshless method with an efficient algorithm for solving obstacle problems, known as the active set algorithm, has been employed. Moreover, the error analysis of the presented method has been investigated. In fact, the main objective of this paper is to demonstrate that the RPIM as a globally weak form method that, just as it has been useful for solving PDE problems, can also be beneficial in solving the obstacle problems.

The outline of the rest of the paper is as follows. In the next section, the active set algorithm for solving the obstacle problem is presented. We will examine the RPIM shape functions and how to use them in global weak form for solving obstacle problem, in the third section. The convergence analysis of the method is presented in the fourth section. In the fifth section, we will provide two numerical examples to assess the efficiency and accuracy of the method.

2 Radial point interpolation method

Consider $\Xi_I = \{\mathbf{x}_l\}_{l=1}^{N_I} \subset D$ and $\Xi_b = \{\mathbf{x}_l\}_{l=1}^{N_b} \subset \partial D$ as the selected scattered point in computational domain and its boundary, respectively. By considering $N = N_I + N_b$, set $\Xi = \{\mathbf{x}_l\}_{l=1}^{N} := \Xi_I \cup \Xi_b$. For y, the function which must be approximated, let $\mathbf{y} = \{y_l = y(\mathbf{x}_l)\}_{l=1}^{N}$. The approximation of y at the interested point $\mathbf{x}$ can be defined as [10, 22]

$$y(\mathbf{x}) \approx y^h(\mathbf{x}) := \sum_{l=1}^{N} R_l(\mathbf{x})c_l + \sum_{s=1}^{r} P_s(\mathbf{x})d_s = R^t(\mathbf{x}) \cdot \mathbf{c} + P^t(\mathbf{x}) \cdot \mathbf{d} \tag{3}$$

where $R_l(\mathbf{x})$ are the radial basis functions (RBF), $P_s(\mathbf{x})$ are polynomial basis functions, and c_l and d_s are the unknown coefficients of the approximation. These coefficients can be determined by imposing the approximating function y^h to pass through all scattered points of Ξ. In order to guarantee the uniqueness of the approximation, the following additional conditions are added to the problem:

$$\sum_{l=1}^{N} P_s(\mathbf{x}_l)c_l = 0, \quad \text{for } s = 1, 2, \ldots, r, \tag{4}$$

where P_ss is built using with Pascal's triangle coefficients and a complete basis is usually preferred. Therefore, the interpolating conditions and additional conditions (4) can be summarized in matrix-vector form as the following equation

$$\hat{\mathbf{y}} := \begin{bmatrix} \mathbf{y}(\mathbf{x}) \\ \mathbf{0} \end{bmatrix} = \begin{bmatrix} \mathbf{R} & \mathbf{P} \\ \mathbf{P}^t & \mathbf{0} \end{bmatrix} \begin{bmatrix} \mathbf{c} \\ \mathbf{d} \end{bmatrix} =: \mathbf{M}\hat{\mathbf{c}}, \tag{5}$$

where $\mathbf{y}(\mathbf{x}) := [y(\mathbf{x}_1), y(\mathbf{x}_2), \cdots, y(\mathbf{x}_N)]^t$ and

$$\mathbf{R} := \begin{bmatrix} R_1(\mathbf{x}_1) & R_2(\mathbf{x}_1) & \cdots & R_N(\mathbf{x}_1) \\ R_1(\mathbf{x}_2) & R_2(\mathbf{x}_2) & \cdots & R_N(\mathbf{x}_2) \\ \vdots & \vdots & \ddots & \vdots \\ R_1(\mathbf{x}_N) & R_2(\mathbf{x}_N) & \cdots & R_N(\mathbf{x}_N) \end{bmatrix}, \tag{6}$$

$$\mathbf{P} := \begin{bmatrix} P_1(\mathbf{x}_1) & P_2(\mathbf{x}_1) & \cdots & P_N(\mathbf{x}_1) \\ P_1(\mathbf{x}_2) & P_2(\mathbf{x}_2) & \cdots & P_N(\mathbf{x}_2) \\ \vdots & \vdots & \ddots & \vdots \\ P_1(\mathbf{x}_N) & P_2(\mathbf{x}_N) & \cdots & P_N(\mathbf{x}_N) \end{bmatrix}. \tag{7}$$

Now, by substituting the solution of (5) in (3), the RPIM approximation of the function y in nodal points Ξ can be written as

$$y(\mathbf{x}) \approx y_h(\mathbf{x}) := \left[R^t(\mathbf{x}), P^t(\mathbf{x})\right] \mathbf{M}^{-1}\hat{\mathbf{y}} = \psi^R(\mathbf{x})\mathbf{y}(\mathbf{x}). \tag{8}$$

The functions $\psi^R(\mathbf{x})$ in (8) are called as RPIM shape functions. It is important to note that, since these approximation interpolate the function values y at the nodal values, the RPIM shape functions satisfy the delta Kronecker property.

Now, we can use the obtained RPIM shape functions as the trail and test functions in the standard Galerkin method. The delta Kronecker property of these functions causes that the boundary conditions can be applied without the need of any other method.

3 Obstacle Problem

Consider the optimization problem

$$\min_{y\in\mathscr{O}} E(y) := \int_D \left(\frac{1}{2}|\nabla y(\mathbf{x})|^2 - g(\mathbf{x})y(\mathbf{x})\right) d\mathbf{x}. \tag{9}$$

It can be shown that (9) has a unique solution which must solve the variational inequality (2) [8]. On the other hand, it's solution must satisfy a strong form which can be obtained as follows.

Consider the point $\mathbf{x}_0$ such that $y(\mathbf{x}_0) < z(\mathbf{x}_0)$. We can find a number $\varepsilon > 0$ and a neighborhood like $N(\mathbf{x}_0)$ where $y(\mathbf{x}) < z(\mathbf{x}) - \varepsilon$ for all $\mathbf{x} \in N(\mathbf{x}_0)$. Let $\varphi \in C^\infty(N(\mathbf{x}_0))$ and $\|\varphi\|_\infty \leq 1$. So, by taking $u = y \pm \varepsilon\varphi$, we have $-\Delta y(\mathbf{x}_0) - g(\mathbf{x}_0) = 0$. Then, consider $\phi \in C^\infty(D)$, $\phi|_{\partial D} = 0$ and $\phi \geq 0$. By substitution of $u = y + \phi$ in (2), we have

$$\int_D (\nabla y(\mathbf{x}).\nabla\phi(\mathbf{x}) - g(\mathbf{x})\phi(\mathbf{x}))\, d\mathbf{x} \leq 0. \tag{10}$$

The differential inequality

$$-\Delta y(\mathbf{x}) - g(\mathbf{x}) \leq 0,\ \mathbf{x} \in D. \tag{11}$$

is the strong form of (10). Therefore, we can write the following strong form complementarity problem as the obstacle problem:

$$-\Delta y(\mathbf{x}) - g(\mathbf{x}) \leq 0,\ \mathbf{x} \in D, \tag{12a}$$

$$y(\mathbf{x}) \leq z(\mathbf{x}),\ \mathbf{x} \in D, \tag{12b}$$

$$(-\Delta y(\mathbf{x}) - g(\mathbf{x}))\,(y(\mathbf{x}) - z(\mathbf{x})) = 0,\ \mathbf{x} \in D, \tag{12c}$$

$$y(\mathbf{x}) = y_b(\mathbf{x}),\ \mathbf{x} \in \partial D. \tag{12d}$$

As a result of rewriting of obstacle problem in (12) form, it can be proved that the computational domain must be divided into two sections [5]. First, the contact region, is denoted by $\mathscr{A}$, where the elastic membrane will collide with the obstacle. It means that in contact region, (12b) holds in the equality form and (12a) holds in the strict inequality form. Latter, the non-contact region, which is denoted by $\mathscr{B}$, where the Poisson equation applies. In other word, in non-contact region (12a) holds in the equality form and (12b) holds in the strict inequality form.

In the first view, one can use (1) and (2) for Galerkin discretization and define the weak form of the discretized obstacle problem, by considering finite dimensional subspace $V_h \subset H^1(D)$, as follows:

$$\text{Find } y_h \in \mathscr{O}_h \subset V_h \subset H^1(D) \tag{13a}$$

$$\langle Ay_h - g_h, y_h - u_h\rangle \leq 0 \quad \forall u_h \in \mathscr{O}_h \tag{13b}$$

but it is important to note that $V_h \subset H^1(D)$ and $\mathscr{O}_h \subset V_h$ cannot yield $\mathscr{O}_h \subset \mathscr{O}$ [5]. For this very reason, we use equations (12a)-(12d) to obtain a discrete weak form for the obstacle problem.

In [12], by defining a the Lagrange function $\lambda(x)$, it had been proven that the solution of CP (12a)-(12c) satisfy the following regularization conditions

$$g(\mathbf{x}) = -\Delta y(\mathbf{x}) + \lambda(\mathbf{x}) \tag{14a}$$

$$\lambda(\mathbf{x}) := \max\{\lambda(\mathbf{x}) + \eta(y(\mathbf{x}) - z(\mathbf{x})), 0\} \tag{14b}$$

where $\eta > 0$ is an arbitrary positive number. It is important to note that, since the max operator in (14b) is non-differentiable operator, the regularized system of equations (14) cannot be solved by usual algorithms that use derivatives. However, this equivalent form of obstacle problem is the base of some numerical methods for solving of the problem. One of the famous method of this family is the active set method, which which will be explained bellow.

The algorithm is initialized with choosing $y^{(0)} = z$ and $\lambda^{(0)} = g + \Delta y^{(0)} \geq 0$. Let $y^{(l)}$ and $\lambda^{(l)}$ be the solution and Lagrange functions obtained in the l-th iteration of the active set algorithm, respectively. The contact and the non-contact set of each iterate can be defined as:

$$\mathscr{A}^{(l+1)} = \{\mathbf{x} \in D |\ \lambda^{(l)}(\mathbf{x}) + \eta(y^{(l)}(\mathbf{x}) - z(\mathbf{x})) > 0\}, \tag{15a}$$

$$\mathscr{B}^{(l+1)} = \{\mathbf{x} \in D |\ \lambda^{(l)}(\mathbf{x}) + \eta(y^{(l)}(\mathbf{x}) - z(\mathbf{x})) \leq 0\}. \tag{15b}$$

By these definitions, the unknown functions must be updated in the following form:

$$y^{(l+1)}(\mathbf{x}) = \mathbf{z}(\mathbf{x}),\ \lambda^{(l+1)}(\mathbf{x}) = g(\mathbf{x}) + \Delta y^{(l+1)}(\mathbf{x}),\ \text{for } \mathbf{x} \in \mathscr{A}^{(l+1)}, \tag{16}$$

$$\lambda^{(l+1)}(\mathbf{x}) = 0,\ -\Delta y^{(l+1)}(\mathbf{x}) = g(\mathbf{x}),\ \text{for } \mathbf{x} \in \mathscr{B}^{(l+1)}. \tag{17}$$

This successive iteration continues until the stopping condition is met as $\mathscr{B}^{(l)} = \mathscr{B}^{(l+1)}$. In the modified version of the active set method, the way of updating in the contact region is changed. In this algorithm, instead of equations (16), one can update $\mathscr{A}^{(l+1)}$ in the following form:

$$\lambda^{(l+1)}(\mathbf{x}) = \lambda^{(l)}(\mathbf{x}) + \eta(y^{(l)}(\mathbf{x}) - z(\mathbf{x})), \tag{18a}$$

$$\Delta y^{(l+1)}(\mathbf{x}) = \lambda^{(l+1)}(\mathbf{x}) - g(\mathbf{x}). \tag{18b}$$

In fact, in the modified active set method the change that has been made is that the Lagrange multiplier is updated before the unknown function y.

4 Radial point interpolation method for obstacle problem

In this section, we purpose RPIM for obstacle problem. To do that, we should use RPIM shape functions in element-free Galerkin scheme as the test and trial functions.

Consider the associated indices with Ξ_I and Ξ_b points with Λ_I and Λ_b, respectively and set $\Lambda = \Lambda_I \cup \Lambda_b$. Denote the mass matrix with $\mathbf{M} := [M(\psi_l, \psi_k)]_{l,k \in \Lambda_I}$ and $\mathbf{g} := [g_k]_{k \in \Lambda_I}$, whose elements are defined as

$$M(\psi_l, \psi_k) := \int_D \nabla \psi_l(\mathbf{x}) \nabla \psi_k(\mathbf{x}) d\mathbf{x}, \tag{19}$$

$$g_k := \int_D g(\mathbf{x}) \psi_k(\mathbf{x}) d\mathbf{x} - \sum_{l \in \lambda_b} M(\psi_l, \psi_k) y_b(\mathbf{x}_k). \tag{20}$$

Now, we can define the RPIM discretization of the obstacle problem as the following discreted complementarity problem:

$$(y_l - z_l)\left(\sum_{l\in\Lambda_I} M(\psi_l,\psi_k)y_l - g_k\right) = 0,\ \mathbf{x}_k \in D, \tag{21a}$$

$$\sum_{l\in\Lambda_I} M(\psi_l,\psi_k)y_l - g_k \leq 0,\ \mathbf{x}_k \in D, \tag{21b}$$

$$y_k - z_k \leq 0,\ \mathbf{x}_k \in D, \tag{21c}$$

$$y_k = y_b(\mathbf{x}_k),\ \mathbf{x}_k \in \partial D, \tag{21d}$$

where $z_k := z(\mathbf{x}_k)$. By considering $\mathbf{z} := [z_k]_{k\in\Lambda_I}$, the matrix-vector form of (21a)-(21c) is as follows:

$$(\mathbf{My} - \mathbf{g}) \odot (\mathbf{y} - \mathbf{z}) = \mathbf{0}, \tag{22}$$

$$\mathbf{My} - \mathbf{g} \leq \mathbf{0}, \tag{23}$$

$$\mathbf{y} - \mathbf{z} \leq \mathbf{0}. \tag{24}$$

where $\odot$ is Hadamard product symbol.

Now, by defining a suitable Lagrange variables we can rewrite these inequalities as equality form. Considering $\boldsymbol{\lambda}$ as Lagrange variables vector, yields that the solution of (24) satisfy the following conditions [12]:

$$\mathbf{My} + \boldsymbol{\lambda} = \mathbf{g}, \tag{25a}$$

$$\boldsymbol{\lambda} = \max\{\boldsymbol{\lambda} + \eta(\mathbf{y} - \mathbf{z}), 0\}, \tag{25b}$$

where η is any positive number.

The equations (25a)-(25b) are RPIM discritized form of (14a)-(14b). Therefore, the modified active set strategy can be implemented in this case.

By considering $\mathbf{y}^{(l)}$ and $\boldsymbol{\lambda}^{(l)}$ as the solution and Lagrange variable in l-th iterate, the algorithm is initialized with $\mathbf{y}^{(0)} = \mathbf{z}$ and $\boldsymbol{\lambda}^{(0)} \geq 0$. Then, all the indices are divided into two disjoint parts:

$$\Lambda_c^{(l)} = \{j \in \Lambda_I |\ \boldsymbol{\lambda}^{(l)} + \eta(\mathbf{y}^{(l)} - \mathbf{z}) > 0\}, \tag{26}$$

$$\Lambda_n^{(l)} = \{j \in \Lambda_I |\ \boldsymbol{\lambda}^{(l)} + \eta(\mathbf{y}^{(l)} - \mathbf{z}) = 0\}. \tag{27}$$

Then, the following new updated variables are considered:

$$\boldsymbol{\lambda}_i^{(l+1)} = 0,\ \text{for } i \in \Lambda_c^{(l)}, \tag{28}$$

$$\mathbf{y}_i^{(l+1)} = \mathbf{z}_i,\ \text{for } i \in \Lambda_n^{(l)}, \tag{29}$$

and by using the sub-matrix notation, for example $\mathbf{M_{nc}}$ for $[\mathbf{M}_{i,j}]_{i\in\Lambda_n^{(l)}, j\in\Lambda_c^{(l)}}$, the remaining variables updated by solving the following linear system

$$\mathbf{M_{nn}}\mathbf{y_n}^{(l+1)} = \mathbf{g_n} + \mathbf{M_{nc}}\mathbf{z_c}, \tag{30}$$

$$\boldsymbol{\lambda}_\mathbf{c}^{(l+1)} = \mathbf{g_c} - \mathbf{M_{cc}}\mathbf{z_c} - \mathbf{M_{cn}}\mathbf{y_n}^{(l+1)}. \tag{31}$$

The algorithm continues until the stopping condition is met as $\Lambda_n^{(l)} = \Lambda_n^{(l+1)}$. The algorithm can be followed in the below steps:

Algorithm 1 Modified active set algorithm

1. Initialized with $\mathbf{y}^{(0)} = \mathbf{z}$ and $\boldsymbol{\lambda}^{(0)} \geq 0$.
2. Divide the computational indices into

$$\Lambda_c^{(l)} = \{j \in \Lambda_I | \, \boldsymbol{\lambda}^{(l)} + \eta(\mathbf{y}^{(l)} - \mathbf{z}) > 0\}, \tag{32}$$

$$\Lambda_n^{(l)} = \{j \in \Lambda_I | \, \boldsymbol{\lambda}^{(l)} + \eta(\mathbf{y}^{(l)} - \mathbf{z}) = 0\}, \tag{33}$$

3. Update variables as

$$\boldsymbol{\lambda}_i^{(l+1)} = 0, \text{ for } i \in \Lambda_c^{(l)}, \tag{34}$$

$$\mathbf{y}_i^{(l+1)} = \mathbf{z}_i, \text{ for } i \in \Lambda_n^{(l)}, \tag{35}$$

4. Compute remained variables by solving the following linear system

$$\mathbf{M_{nn}}\mathbf{y_n}^{(l+1)} = \mathbf{g_n} + \mathbf{M_{nc}}\mathbf{z_c}, \tag{36}$$

$$\boldsymbol{\lambda}_\mathbf{c}^{(l+1)} = \mathbf{g_c} - \mathbf{M_{cc}}\mathbf{z_c} - \mathbf{M_{cn}}\mathbf{y_n}^{(l+1)}. \tag{37}$$

5. Repeat steps 2-4 until the following condition is met.

$$\Lambda_n^{(l)} = \Lambda_n^{(l+1)}. \tag{38}$$

4.1 Error analysis of the presented method

It has been proven that under the given assumptions the active set algorithm is uniformly convergent, and if it stops under the considered stopping condition, the obtained solution satisfy (25a) and (25b) [12].

Let $h = h(\Xi, D)$ be fill distance of D, i.e. [11]

$$h(\Xi, D) = \sup_{\mathbf{x}\in D} \min_{\mathbf{x}_l \in \Xi} \|\mathbf{x} - \mathbf{x}_l\|_2.$$

In fact, the density of the computational points in the domain D can be measured by $h(\Xi, D)$. Consider y as the analytical solution of obstacle problem (12). Moreover, $y^{(l)}$ is the analytical solutions obtained by active set strategy and $y_h^{(l)}$ is the numerical solutions of RPIM implementation. It means that

$$y_h^{(l)}(\mathbf{x}) = \psi^R(\mathbf{x})\mathbf{y}^{(l)} = \sum_{k=1}^{N} \psi_k(\mathbf{x}) y_k,$$

where $\psi^R = [\psi_1, \psi_2, \ldots, \psi_N]^t$.

Lemma 1. *[12] Let $z \geq y^{(0)} \geq y$ be given. By defining $\lambda^{(0)} = \max\{g - A\}$, Algorithm 1 converges monotonically. It means that $y \leq y^{(l+1)} \leq y^{(l)}$, for all $l \geq 0$.*

Theorem 1. *The modified active set algorithm described in Algorithm 1 is convergent in the H^1 norm to the analytical solution of the obstacle problem (12).*

Proof. First, we can write

$$\begin{aligned}\int_D \left[\Delta y^{(l+1)} - \Delta y\right]^2 dx &= \int_D \left[\Delta y^{(l+1)} - \Delta y^{(l)} - c(y^{(l)} - z) + \Delta y^{(l)} + c(y^{(l)} - z) - \Delta y\right]^2 dx \\ &= \int_D \left[\Delta y^{(l)} + c(y^{(l)} - z) - \Delta y\right]^2 - \left[\Delta y^{(l+1)} - \Delta y^{(l)} - c(y^{(l)} - z)\right]^2 \\ &\quad + 2\left[\Delta y^{(l+1)} - \Delta y^{(l)} - c(y^{(l)} - z)\right] \cdot \left[\Delta y^{(l+1)} - \Delta y\right] dx. \end{aligned} \tag{39}$$

First, for any $x \in \mathscr{B}^{(l+1)}$, we have $0 \geq \lambda^{(l)}(x) + c(y^{(l)}(x) - z(x)) = \Delta y^{(l)}(x) - g(x) + c(y^{(l)}(x) - z(x))$. Substituting $g(x) = -\Delta y^{(l+1)}(x)$ from (17) leads to $\Delta y^{(l+1)}(x) - \Delta y^{(l)}(x) - c(y^{(l)}(x) - z(x)) \geq 0$. On the other hand, for any $x \in \mathscr{A}^{(l+1)}$, according to (18b) we have $\lambda^{(l+1)}(x) - \lambda^{(l)}(x) - c(y^{(l)}(x) - z(x)) = \Delta y^{(l+1)}(x) - \Delta y^{(l)}(x) - c(y^{(l)}(x) - z(x)) = 0$.

Now, since inequality $-\Delta y(x) \leq g(x)$ holds for the exact solution y, by substituting $g(x) = -\Delta y^{(l+1)}(x)$, we have $\Delta y^{(l+1)}(x) - \Delta y(x) \leq 0$. It concludes that

$$\int_D \left[\Delta y^{(l+1)} - \Delta y^{(l)} - c(y^{(l)} - z)\right]\left[\Delta y^{(l+1)} - \Delta y\right] dx \leq 0. \tag{40}$$

By combining results (39) and (40), we get the following inequalities

$$\begin{aligned}\|\Delta y^{(l+1)} - \Delta y\|^2 &\leq \int_D \left[\Delta y^{(l)} - \Delta y\right]^2 - \left[\Delta y^{(l+1)} - \Delta y^{(l)}\right]^2 + 2c(y^{(l)} - z) \cdot \left[\Delta y^{(l+1)} - \Delta y\right] dx \\ &= \|\Delta y^{(l)} - \Delta y\|^2 - \|\Delta y^{(l+1)} - \Delta y^{(l)}\|^2 + 2c\int_D (y^{(l+1)} - y) \cdot \left[\Delta y^{(l+1)} - \Delta y\right] dx \\ &\quad + 2c\int_D (y^{(l+1)} - y^{(l)}) \cdot \left[\Delta y - \Delta y^{(l+1)}\right] + (y - z) \cdot \left[\Delta y^{(l+1)} + g\right] dx \\ &\quad - 2c\int_D (y - z) \cdot [\Delta y + g]\, dx. \end{aligned} \tag{41}$$

Applying Gauss theorem for the first integral in right hand side of (41) leads to

$$\int_D (y^{(l+1)} - y) \cdot \left[\Delta y^{(l+1)} - \Delta y\right] dx = -\int_D \left[\nabla y^{(l+1)} - \nabla y\right]^2 dx. \tag{42}$$

Moreover, the value of the second integral is negative and the third integral will vanish since complementarity condition (12d) holds. Thus, we can conclude that

$$\|\Delta y^{(l+1)} - \Delta y\|^2 \leq \|\Delta y^{(l)} - \Delta y\|^2 - \|\Delta y^{(l+1)} - \Delta y^{(l)}\|^2 \leq \|\Delta y^{(l)} - \Delta y\|^2. \tag{43}$$

Consequently, (43) yields that $\lim_{l\to\infty} \Delta y^{(l)} = \Delta y$. So, by considering (42), we can obtain $\lim_{l\to\infty} |\nabla y^{(l)} - \nabla y| = 0$. Finally, by combining the letter result and the result of Lemma 1, we can conclude that $\lim_{l\to\infty} \|y^{(l)} - y\|_{H^1(D)} = 0$ and the proof is completed. □

In [25] the error estimate of RPIM approximation has been discussed and the following theorem is given for interpolating by multiquadric RBFs.

Lemma 2. *[25] The error of interpolation by multiquadric RBFs $\phi(r) = \left(\alpha^2 + r^2\right)^{\frac{s}{2}}$, for all functions $y : \mathbb{R}^n \to \mathbb{R}$ with generalized Fourier transform $\hat{Y}$ satisfying in*

$$\int_D |\hat{Y}|^2 \|t\|^{n+s} exp(\|t\|) dt < \infty,$$

is

$$|y^{(m)}(\mathbf{x}) - y_h^{(m)}(\mathbf{x})| \leq C \cdot c_y \cdot h^{k-|m|}(\mathbf{x}),$$

where $0 \leq |m| \leq k$ and $|m| = \sum_l m_l$. Here,

$$c_y = \frac{1}{(2\pi)^n} \int_D |\hat{Y}(t)|^2 (\hat{\psi}(t))^{-1} dt < \infty.$$

5 Numerical illustrations

This section is devoted to solve various numerical examples of obstacle problem with the presented RPIM method. Computer programming was done in MATLAB software, and was executed on a personal computer. This PC has a 3. Giga-Hertz Core i5 Processor and 8 Gbs of RAM.

The multiquadric RBFs which are used in constructing RPIM shape functions, are defined as follows

$$R_k(\mathbf{x}) = \left((\alpha h)^2 + \|\mathbf{x} - \mathbf{x}_k\|^2\right)^s, \tag{44}$$

where the radius of the local support domain is considered as $r_l = \alpha_l h$. Regarding the selection of parameters α and s, we note that in reference [20], the corresponding values of these parameters are stated as $\alpha = 1 \sim 7$ and $s = 1.03$, respectively.

We have used the composite Gaussian quadrature to calculate all integrals in the algorithm. More precisely, first we divided the integration domain into several separated subdomains and then we used a Gaussian integration formula in each subdomain. In the following examples, the number of subdomains in the integral regions is 16 and the 8-point Gauss-Lobatto-Legendre formula is used in each subdomain. One area of future research could be research into more appropriate integration methods for numerically solving the integrals in the method. Because, in this method, increasing nodes in Gauss quadrature rules, not only greatly increase the computational cost, but also impair the optimal convergence.

Example 1. Our first example is devoted to a two-dimensional obstacle problem with forcing function $z(\mathbf{x}) = 0$ and obstacle function as $g(\mathbf{x}) = 2$. This problem defined in $D = [-1.5, 1.5]^2$. It has the unique exact solution as follows [17]:

$$y^*(\mathbf{x}) = \begin{cases} \ln\sqrt{x_1^2 + x_2^2} - \frac{x_1^2 + x_2^2 - 1}{2}, & \text{for } \sqrt{x_1^2 + x_2^2} \geq 1, \\ 0, & \text{for } \sqrt{x_1^2 + x_2^2} < 1. \end{cases}$$

It had be proven that the contact region is the unit disc $x_1^2 + x_2^2 \leq 1$.

The obtained solution by applying RPIM with $h = \frac{1}{20}$, $\alpha = 5$ and $\alpha_l = 4$ is plotted in Figure 1. Moreover, Figure 2 shows the gridpoints that the described algorithm has identified as the contact or the non-contact points.

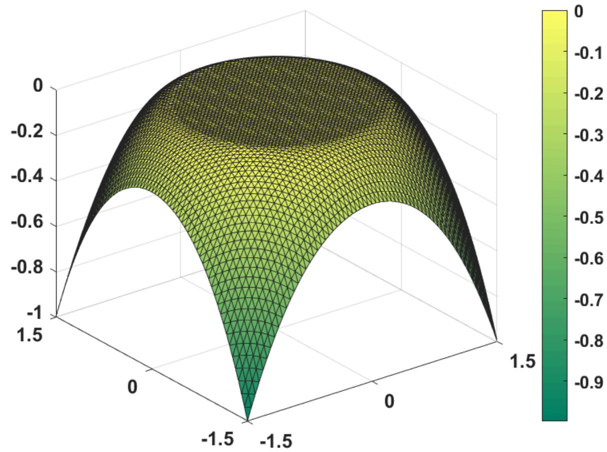

Figure 1: The solution function for Example 1 by using RPIM with $h = \frac{1}{20}$, $\alpha = 5$ and $\alpha_l = 4$.

Also, Table 1 contains L_2-error of the presented method for different choices of h and α. In this table, the computational order of error is calculated by the following formula:

$$order = \frac{\log(E_1) - \log(E_2)}{\log(h_1) - \log(h_2)}, \tag{45}$$

where E_1 and E_2 are the errors associated with h_1 and h_2, respectively.

Table 1: The computed errors and the computational order of error for Example 1.

	$\alpha = 4$		$\alpha = 5$		$\alpha = 6$	
h	$\|y^* - y_h\|_2$	order	$\|y^* - y_h\|_2$	order	$\|y^* - y_h\|_2$	order
0.2	$4.8931e-02$	–	2.5704e-02	–	2.1417e-02	–
0.1	$1.5132e-02$	1.6931	7.2241e-03	1.8311	5.2147e-03	2.0381
0.05	$4.1021e-03$	1.8832	1.9124e-03	1.9174	1.0622e-03	2.2955
0.02	$7.1656e-04$	1.9042	3.1922e-04	1.9538	1.1986e-04	2.3811

Example 2. In this example, the computational domain is $D = (-2,2) \times (-2,2)$ and the obstacle function is defined as follows

$$g(\mathbf{x}) = \begin{cases} \sqrt{1-r^2}, & \text{for } r \le 1, \\ -1, & \text{o.w.} \end{cases}$$

where $r = \|\mathbf{x}\|_2 = \sqrt{x_1^2 + x_2^2}$. The forcing function g is set equal to zero on D. In this example, the Dirichlet boundary condition is determined such that the following function is the exact solution of the problem [28]:

$$u^*(x,y) = \begin{cases} \sqrt{1-r^2}, & r \le a, \\ \frac{-a^2}{\sqrt{1-a^2}} \ln(r/2), & r > a. \end{cases}$$

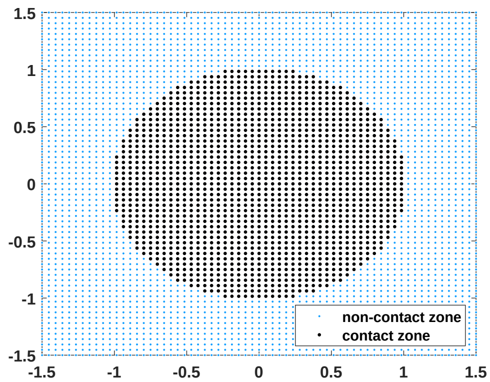

Figure 2: Grid points in contact and non-contact regions for Example 2.

Here $a \in \mathbb{R}$ is less than 1 and being satisfied in $a^2\left(1-\ln(\frac{a}{2})\right)=1$. In this example, the contact zone is a disk of radius a.

The obtained solution by applying RPIM with $h=\frac{1}{20}$, $\alpha=6$ and $\alpha_l=6$ is plotted in Figure 3.

Also, Table 2 contains L_2-error of the presented method with $\alpha_l=6$ and choosing different values of h and α. In this table the computational order of error is reported in term of (45). Table 3 shows the results of the presented method in comparison with some other methods.

Table 2: The computed errors and the computational order of error for Example 2.

	$\alpha=4$		$\alpha=5$		$\alpha=6$	
h	$\|y^*-y_h\|_2$	order	$\|y^*-y_h\|_2$	order	$\|y^*-y_h\|_2$	order
0.2	$3.3705e-02$	–	2.1751e-02	–	1.5301e-02	–
0.1	$9.4178e-03$	1.8395	5.8881e-03	1.8852	3.7849e-03	2.0153
0.05	$2.5240e-03$	1.8997	1.5615e-03	1.9149	8.1601e-04	2.2136
0.02	$4.3642e-04$	1.9153	2.6459e-04	1.9374	8.7401e-05	2.438

The results compared with direct local boundary integral equation method (DLBIE) , the element free Galerkin method (EFG) and Interpolation element free Galerkin method (IEFG). The results indicate the appropriate accuracy of the proposed method for solving the obstacle problem.

Table 3: Absolute errors of some meshless methods for Example 2.

h	RPIM	DLBIE	EFG	IEFGM
0.2	$1.5301e-02$	6.531e-02	2.0613e-02	4.9142e-02
0.1	$3.7849e-03$	1.7438e-02	4.1772e-03	6.5011e-03
0.05	$8.1601e-04$	5.0721e-03	3.1995e-03	3.4821e-03
0.02	$8.7401e-05$	7.4271e-04	2.3140e-04	1.7112e-04

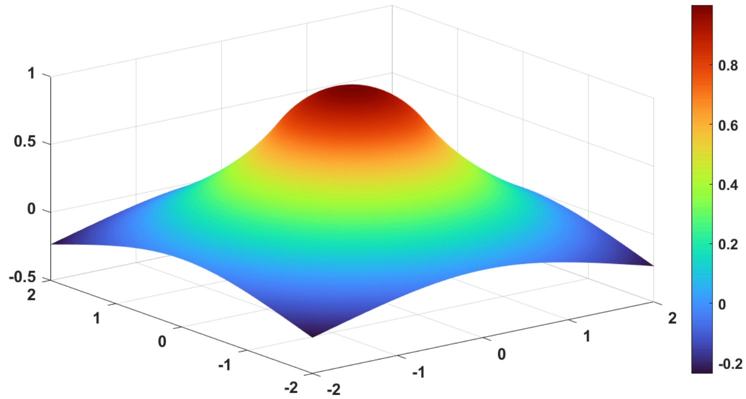

Figure 3: The solution function for Example 2 by using RPIM with $h = \frac{1}{20}$, $\alpha = 6$ and $\alpha_l = 6$.

6 Conclusion

In this paper, a mesh-less method based on radial point interpolation method is presented for numerical solving of the obstacle problem. This method is combined with the active set algorithm to be suitable for solving elliptic variational inequality problems such as the obstacle problem. Some results about convergence of the presented method has been proven and finally, two examples of obstacle problems have been solved by the presented method. The calculated results showed that the RPIM is efficient and it can provides accurate solution for the obstacle problem.

References

[1] M. Abbaszadeh, H. Pourbashash, M. Khaksar-e Oshagh, *The local meshless collocation method for solving 2d fractional klein-kramers dynamics equation on irregular domains*, Int. J. Numer. Methods Heat Fluid Flow. **32** (2022) 41–61.

[2] L. Banz, A. Schröder, *Biorthogonal basis functions in hp-adaptive fem for elliptic obstacle problems*, Comput. Math. Appl. **70** (2015) 1721–1742.

[3] E. Burman, P. Hansbo, M. G. Larson, R. Stenberg, *Galerkin least squares finite element method for the obstacle problem*, Comput. Methods Appl. Mech. Eng. **313** (2017) 362–374.

[4] H.F. Chan, C. M. Fan, C. W. Kuo, *Generalized finite difference method for solving two-dimensional non-linear obstacle problems*, Eng. Anal. Bound. Elem. **37**(2013) 1189–1196.

[5] C. Grossmann, H.G. Roos, M. Stynes, *Numerical treatment of partial differential equations*, Springer, 2007.

[6] A. Goligerdian, M.K. Oshagh, M. Jaberi-Douraki, *Applying thin plate splines to the Galerkin method for the numerical simulation of a nonlinear model for population dynamics*, J. Comput. Appl. Math. **451** (2024) 116036.

[7] M. Hintermüller, K. Ito, K. Kunisch, *The primal-dual active set strategy as a semismooth newton method*, SIAM J. Optim. **13** (2002) 865–888.

[8] V. Hrynkiv, *Optimal Control of Partial Differential Equations and Variational Inequalities*, The University of Tennessee, 2006.

[9] M. Ilati, *Analysis and application of the interpolating element-free galerkin method for extended Fisher–Kolmogorov equation which arises in brain tumor dynamics modeling*, Numer. Algorithms. **85**(2020) 485–502.

[10] M. Jalalian, K.W. Ali, S.R. Qadir, M. Jalalian, *A numerical method based on the radial basis functions for solving nonlinear two-dimensional volterra integral equations of the second kind on non-rectangular domains*, J. Math. Model. **12** (2024) 687–705.

[11] M. Jalili, R. Salehi, *The approximate solution of one dimensional stochastic evolution equations by meshless methods*, J. Math. Model. **9** (2021) 599–609.

[12] T.Kärkkäinen, K.Kunisch, P.Tarvainen, *Augmented lagrangian active set methods for obstacle problems*, J. Optim. Theory Appl. **119** (2003) 499–533.

[13] M. Khaksar-e Oshagh, M. Shamsi, *An adaptive wavelet collocation method for solving optimal control of elliptic variational inequalities of the obstacle type*, Comput. Math. Appl. **75** (2018) 470–485.

[14] M. Khaksar-e Oshagh, M. Shamsi, M. Dehghan, *A wavelet-based adaptive mesh refinement method for the obstacle problem*, Eng. Comput. **34** (2018) 577–589.

[15] M. Khaksar-e Oshagh, M. Shamsi, *Direct pseudo-spectral method for optimal control of obstacle problem–an optimal control problem governed by elliptic variational inequality*, Math. Methods Appl. Sci. **40** (2017) 4993–5004.

[16] T. Lewis, A. Rapp, Y. Zhang, *Convergence analysis of symmetric dual-wind discontinuous galerkin approximation methods for the obstacle problem*, J. Math. Anal. Appl. **485** (2020) 123840.

[17] R. Li, W. Liu, T. Tang, *Moving Mesh Finite Element Approximations for Variational Inequality I: Static Obstacle Problem*, Hong Kong Baptist University, Hong Kong, 2000.

[18] X. Li, H. Dong, *An element-free galerkin method for the obstacle problem*, Appl. Math. Lett. **112** (2021) 106724.

[19] X.P. Lian, Z. Cen, X.L. Cheng, *Some iterative algorithms for the obstacle problems*, Int. J. Comput. Math. **87** (2010) 2493–2502.

[20] G.R. Liu, Y. Gu, *An introduction to meshfree methods and their programming*, Springer Science & Business Media, 2005.

[21] G. Liu, Y. Gu, *A point interpolation method for two-dimensional solids*, J. Numer. Methods Eng. **50** (2001) 937–951.

[22] H. Pourbashash, M. Khaksar-e Oshagh, *Local RBF-FD technique for solving the two-dimensional modified anomalous sub-diffusion equation*, Appl. Math. Comput. **339** (2018) 144-152.

[23] H. Pourbashash, M. Khaksar-e Oshagh, S. Asadollahi, *An efficient adaptive wavelet method for pricing time-fractional american option variational inequality*, Comput. Methods Differ. Equ. **12** (2024) 173–188.

[24] M. Ulbrich, *Semismooth Newton methods for variational inequalities and constrained optimization problems in function spaces*, SIAM, 2011.

[25] Z. Wu, R. Schaback, *Local error estimates for radial basis function interpolation of scattered data*, IMA J. Numer. Anal. **13** (1993) 13–27.

[26] J. Xiao, M. McCarthy, *Meshless analysis of the obstacle problem for beams by the mlpg method and subdomain variational formulations*, Eur. J. Mech. A Solids **22** (2003) 385–399.

[27] M. Yaghouti, H. Ramezannezhad Azarboni, *Determining optimal value of the shape parameter c in RBF for unequal distances topographical points by cross-validation algorithm*, J. Math. Model. **5** (2017) 53–60.

[28] D. Yuan, X. Cheng, *A meshless method for solving the free boundary problem associated with unilateral obstacle*, Int. J. Comput. Math. **89** (2012) 90–97.

[29] J. X. Zhao, S. Wang, *An interior penalty approach to a large-scale discretized obstacle problem with nonlinear constraints*, Numer. Algorithms. **85** (2020) 571–589.

[30] M. Zhao, H. Wu, C. Xiong, *Error analysis of hdg approximations for elliptic variational inequality: obstacle problem*, Numer. Algorithms. **81** (2019) 445–463.